Volume 1
Number 4
August 2025
Pages 655-988

EES Batteries

rsc.li/EESBatteries

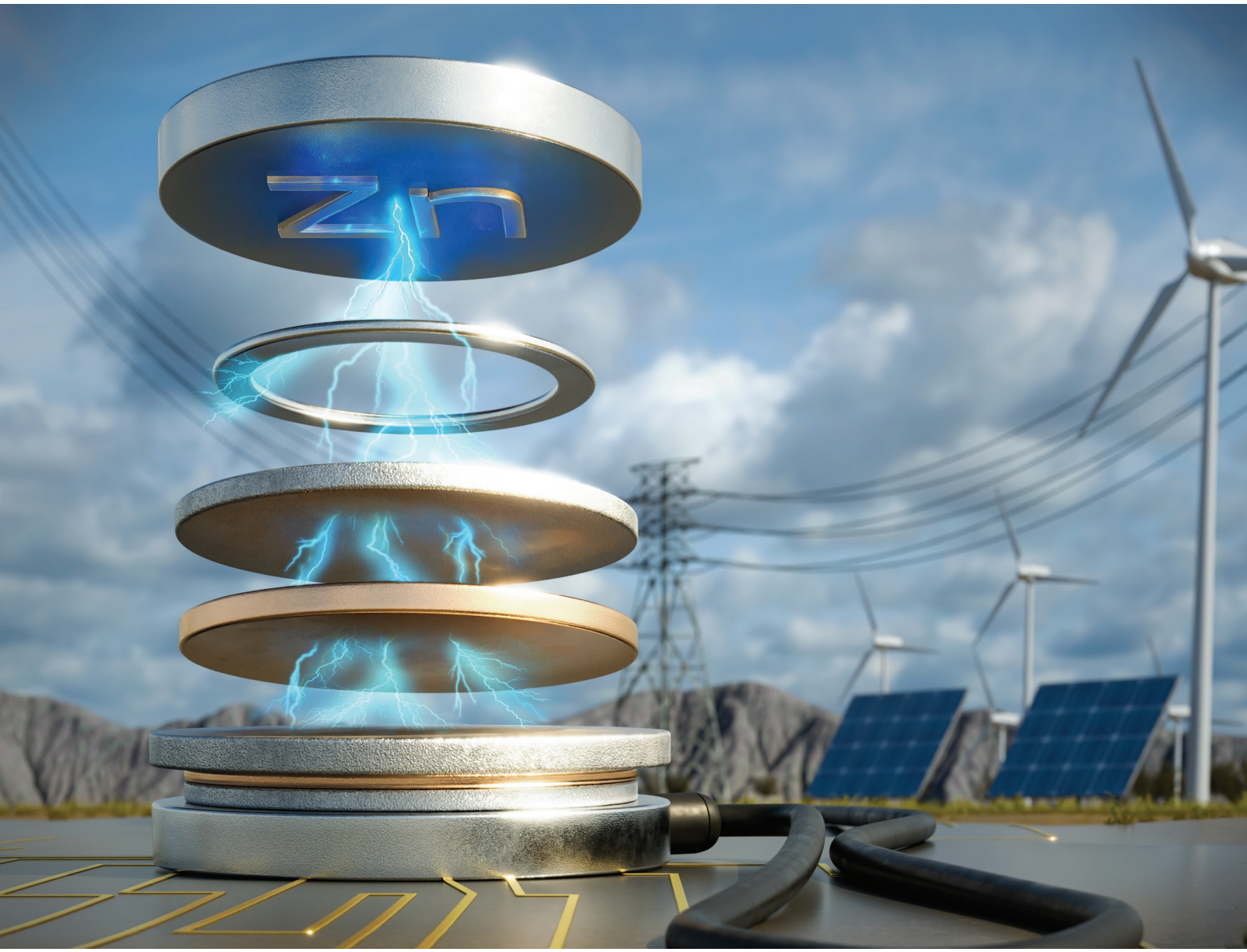

ISSN 3033-4071

ROYAL SOCIETY OF CHEMISTRY

PAPER
Jeffrey E. Dick *et al.*
Small changes, big gains: standardizing non-electrode coin cell components in aqueous zinc battery research

EES Batteries

ROYAL SOCIETY OF CHEMISTRY

PAPER

View Article Online
View Journal | View Issue

Check for updates

Cite this: *EES Batteries*, 2025, **1**, 813

Small changes, big gains: standardizing non-electrode coin cell components in aqueous zinc battery research†

Saptarshi Paul,‡[a] James H. Nguyen,‡[a] Michael L. Harrigan,[a] Ashutosh Rana,[a] Andy Berbille[a] and Jeffrey E. Dick *[a,b]

Aqueous Zinc Metal Batteries (AZMBs) hold the potential for safe and cost-effective solutions for next-generation energy storage. While coin cells are the most used model in lab studies, current literature often overlooks the influence of the non-electrode components, namely the current collector, spacer, spring, and casing materials. The lack of standardization of AZMB coin cells assembly stifles reproducibility, applications, and comparisons across studies. Here, we present a systematic study that reveals the profound impact of these non-electrode components on AZMB performance. We found the optimal coin cell comprises a titanium or copper current collector, stainless steel (SS) components (spacer, spring, and casing) protected by a copper foil, and an electrolyte volume of 40 μL. This optimized AZMB coin cell attains a 99.78% coulombic efficiency (CE), in stark contrast with the 99.3% achieved by a Zn||Cu asymmetric coin cell (control). In addition, these optimizations improve the cyclability by more than 20 times over the control (1950 *vs.* 80 cycles). Despite the straightforward and cost-effective nature of these modifications, their undeniable repercussion on AZMB performance substantiates the importance of moving towards standardized non-electrode coin cell components and assembly protocols in this field. Our study, and proposed standards, enable accurate evaluation and comparisons of the impact of additives, current variations, and other performance-enhancing strategies in AZMB research.

Received 30th April 2025,
Accepted 2nd May 2025

DOI: 10.1039/d5eb00084j

rsc.li/EESBatteries

Open Access Article. Published on 07 1446. Downloaded on 26/08/47 09:31:43 .
This article is licensed under a Creative Commons Attribution 3.0 Unported Licence.

Broader context

As the global energy landscape shifts toward renewable sources, the need for safe, cost-effective, and scalable energy storage solutions has never been greater. Aqueous Zinc Metal Batteries (AZMBs) offer a promising alternative to lithium-ion technology, boasting inherent safety, abundant raw materials, and environmental sustainability. However, a critical yet often overlooked barrier to their development is the lack of standardization in laboratory-scale coin cell assembly, the primary platform for evaluating AZMB performance. Inconsistencies in non-electrode components, such as current collectors, spacers, springs, and casings, obscure meaningful comparisons and hinder the reproducibility essential for scientific progress. Our study directly addresses this challenge by systematically assessing the impact of these components on AZMB electrochemical behavior. By identifying optimal materials and configurations such as utilizing copper current collectors, stainless steel components protected with copper foil, and a controlled electrolyte volume, we demonstrate how small, yet strategic modifications can massively improve coulombic efficiency and cycle life. These findings provide a much-needed framework for standardized coin cell assembly, ensuring that future research yields results that are both reliable and comparable. In doing so, this work accelerates the pathway to practical AZMB deployment.

Introduction

The energy storage sector today faces challenges of material scarcity, safety risks, and environmental concerns.[1–5] Aqueous zinc–metal batteries (AZMBs) offer high capacity (820 mA h g^{-1}), low cost ($65 kW^{-1} h^{-1}),[1,6,7] and environmental compatibility enabled by aqueous electrolytes.[8–11] Mildly acidic electrolytes (pH 3–7) are particularly advantageous for practical AZMB applications by providing superior cycling stability compared to their alkaline counterparts.[12–15] Despite their advantages, AZMBs face commercialization challenges due to para-

[a]*Department of Chemistry, Purdue University, West Lafayette, IN, 47907, USA. E-mail: jdick@purdue.edu*
[b]*Elmore Family School of Electrical and Computer Engineering, Purdue University, West Lafayette, IN, 47907, USA*

†Electronic supplementary information (ESI) available. See DOI: https://doi.org/10.1039/d5eb00084j

‡Denotes equal contribution.

© 2025 The Author(s). Published by the Royal Society of Chemistry

Open Access Article. Published on 07 1446. Downloaded on 26/08/47 09:31:43 .
This article is licensed under a Creative Commons Attribution 3.0 Unported Licence.

sitic reactions during zinc electrodeposition.[16–19] These reactions lead to dendrite growth, corrosion, and passivation, impacting performance. Mitigating strategies including electrolyte additives,[20] adjustment of current density,[21,22] and modification of electrode substrates[23] have shown promising results in improving the performance of the cell. However, among these factors, the influence of non-electrode materials of a coin cell on the performance of AZMB across different studies is not comprehensively addressed in the literature.

The first and primary step toward real-world AZMB applications is rigorous lab research, with stainless-steel coin cells as the primary platform for studying zinc battery systems. Common in lithium-ion and sodium-ion research, coin cells are cost-effective and preferred over alternative configurations.[24–27] Previous studies, such as Kundu's work in 2021[28] and Zhou's in 2023,[29] have focused on improving the coin cell's current collector and spacer configurations, respectively. Similarly, Yang's group extensively evaluated various current collectors in 2023 to optimize their performance.[30] Despite these advances, a comprehensive study examining the impact of the electrodeposition of Zn and consequent side reactions, such as HER, corrosion, and passivation on all the non-electrode components of the coin cell-current collectors, spacers, springs and casing materials as depicted in the above Fig. 1 remains absent in the literature. In Fig. 1(A), we show these non-electrode materials can have potential impact on Zn electrodeposition and as depicted in Fig. 1(B), it will eventually impact the battery performance. Given the substantial impact of these elementary modifications, our findings underscore the urgent need for researchers to report and eventually standardize coin cell assembly details to ensure consistency and meaningful performance comparisons across different kinds of AZMB studies. This knowledge gap is being addressed in our work here.

First, we screen different materials which can be used as prospective current collectors. After examining the prospective current collector's battery performance and observing the effects of Zn electrodeposition, passivation, and corrosion with techniques such as SEM, EDX, and XRD, we show that Ti and Cu yielded similar performance as current collectors and were more efficient than SS and Ni. With this understanding on material performance as current collectors, we go on to add a layer of Cu as a protective foil in front of the SS non-electrode components to diminish the harmful effects of HER, corrosion, and passivation. The results showed that both the coulombic efficiency and cyclability of the coin cell drastically increased. Second, to further minimize the deteriorating effects of the side reactions, we implemented different volumes of the electrolyte as the electrolyte is both responsible for Zn deposition and HER simultaneously as shown recently. We observe that lower amount of electrolyte (40 μL) than what is conventionally used (200 μL) goes to show better performance and cyclability for the battery. All the optimizations we implemented show a higher CE than our standard control Zn||Cu asymmetric coin cell (99.3%), with our most optimized coin cell showing the best performance with 99.78% CE and lasting for 1950 cycles compared to our control which lasted for 80 cycles. These modifications highlight the influence of the non-electrode components of the coin cell and underscore the importance of systematically reporting coin cell assembly protocols, ensuring accurate and meaningful comparisons of battery performance. Without standardization or proper

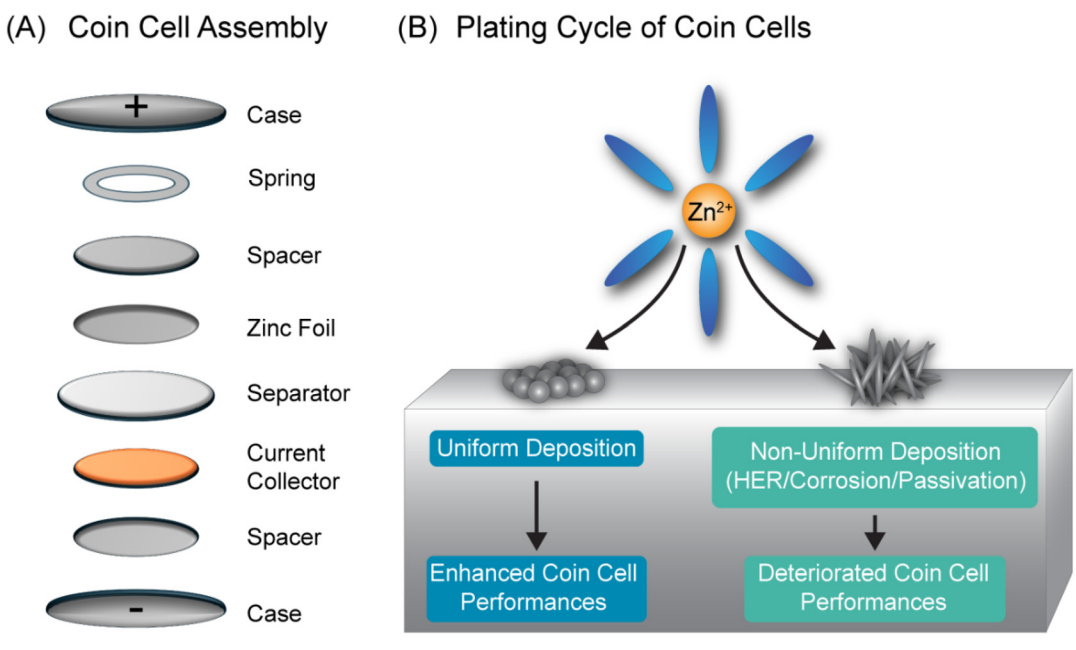

Fig. 1 (A) Schematic depicting different components of a coin cell. (B) Schematic illustrating the impact of Zn electrodeposition and side reactions on battery performance, influenced by various coin cell components.

© 2025 The Author(s). Published by the Royal Society of Chemistry

Open Access Article. Published on 07 1446. Downloaded on 26/08/47 09:31:43 .
This article is licensed under a Creative Commons Attribution 3.0 Unported Licence.

reporting of coin cell assembly, the role of additives, coatings, substrate design, and other performance-enhancing strategies cannot reliably be compared and analysed between studies.

Results and discussion

Optimizing current collector

To evaluate the distribution of charge among various current collectors, we investigated materials such as titanium (Ti), copper (Cu), nickel (Ni), aluminum (Al), and stainless steel (SS).[28] Initially, we assessed the performance of these current collectors using coin cell configuration of Fig. 1(A) with 200 μL of 1 M $ZnSO_4$ electrolyte. Subsequently, we analyzed the charge distribution between zinc electrodeposition and side reactions through detailed characterization using SEM, EDX and XRD.

Fig. 2(A) shows the CE observed for the cycling of Zn asymmetric cells with different current collectors and a fixed current density of 1 mA cm^{-2}, capacity of 0.5 mA h cm^{-2} and a stripping cut off at +0.5 V. The average CE values were calculated using eqn (1).

$$CE_{avg} = \frac{1}{N}\sum\frac{Q_s}{Q_p} \quad (1)$$

where N represents the number of cycles (here, N = 50), Q_s is the stripped charge and Q_p is the plated charge. Fig. 2(A) reveals that Ti and Cu are performing better than Ni and SS (a trend that is frequently observed in this work). Al also shows similar efficiency to Ni here, but the upcoming sections will show its erratic behavior as reported in literature previously.[28] Additionally, Fig. 2(C) shows that the initial coulombic efficiency (ICE) values also indicate the same trend. Along with these two observations, we performed a galvanostatic protocol given by Xu *et al.*[31,32] There is an initial preconditioning cycle that is performed to minimize substrate effects (lattice mismatch and interphase interactions), followed by a constant Zn deposition at 5 mA h cm^{-2} to provide a reservoir of Zn to determine CE (Q_r). Consequently, we chose a capacity of 1 mA h cm^{-2} (Q_c) to cycle the coin cell 9 times prior to stripping, until the potential reaches +0.5 V *vs.* Zn/Zn^{2+}; this ensures all the Zn is stripped off. The current density is constant for the entire protocol. The potential *versus* time curve obtained for Ti, was done by this protocol which can be seen in Fig. 2(B). Ti and Cu outperform Ni and SS and Al also shows appreciable CE. We provide the corresponding curves for Cu, Al, Ni and SS in Fig. S1.† In Fig. 2(D), the same behavior is noted across different measurements. In the following sections, we analyze the charge distribution trend across different materials to determine its underlying cause.

As previously discussed, hydrogen evolution reaction (HER) compromises current collector stability. To assess susceptibility to HER, we tested various current collector materials in 1 M KCl using a platinum counter electrode and measured HER onset potentials against an Ag/AgCl reference electrode.[33–35] Fig. S2† reveals that Ni (green) and SS (purple) are more prone to HER compared to Ti (red) and Cu (yellow). The inset highlights the significant difference in HER onset potential between SS and Ti. This distinction is critical, as Ti demonstrates the highest CE, while SS shows the poorest performance. Al also shows later onset potential to HER supporting its

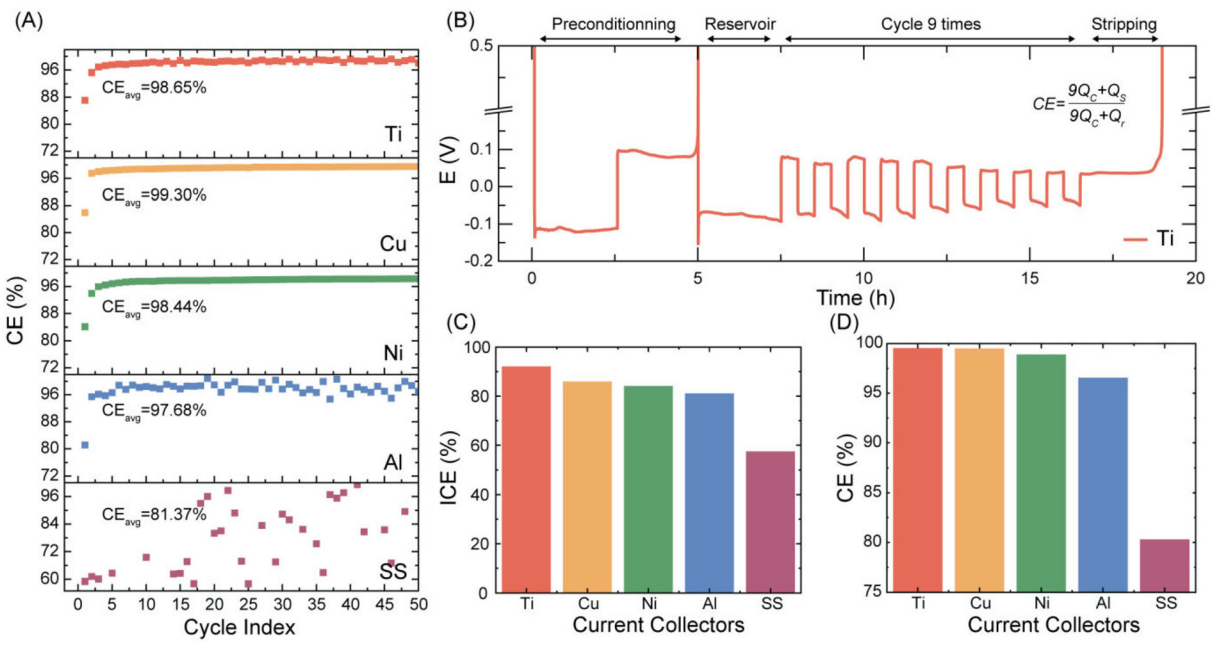

Fig. 2 (A) The Coulombic Efficiency (CE) of asymmetric cells with different current collector materials, over 50 cycles. (B) Representative potential *vs.* time (Aurbach) curve for Ti. (C) Initial Coulombic Efficiency (ICE) trends from the coin cell data. (D) Coulombic efficiency trends using Aurbach curve as shown in (B), as function of current collector materials.

Open Access Article. Published on 07 1446. Downloaded on 26/08/47 09:31:43 .
This article is licensed under a Creative Commons Attribution 3.0 Unported Licence.

performance seen in Fig. 2. In subsequent sections, we further explore how Ti consistently shows superior performance, while SS exhibits suboptimal results across the board. By observing the different onset potentials displayed by the current collectors within the study, we indicate the effect of different current collectors used in a coin cell. Next, we analyze electrodeposition and side reactions affecting their stability.

In this section, we explore the distribution of charge to Zn electrodeposition for the different current collectors. Since, we have observed better CE performance for Ti and Cu than Ni and SS, we expect it to be related to the nucleation of Zn at these current collectors as well. From previous literature it is known that morphology of Zn particles deposited plays a big role in the efficiency of the battery.[36–38] Therefore, to observe this phenomenon and understand the nucleation of Zn on the different current collectors, we do a galvanostatic plating of 0.5 mA h cm^{-2} on Zn using 1 mA cm^{-2} current density for all the current collectors using the asymmetric coin cell setup and 1 M $ZnCl_2$ as the electrolyte. We observe that the nucleation overpotential is more for Ti and Cu than for Ni and SS as shown in Fig. 3(A). This supports our previous performance data as we know from classical nucleation theory that a higher nucleation overpotential results in a higher areal density and smaller critical radius.[39] This directly correlates to having a uniform deposition which should improve the cyclability and performance of the AZMB.

Additionally, we also conducted contact angle studies (goniometry) to learn about the electrodeposition of Zn on the different current collectors. It is known that a lower contact angle means, the surface is more wettable and thus the interfacial energy is lower and should result in a more uniform deposition.[39] This is exactly observed in Fig. S3(A)†, where we analyze the final contact angle of the different current collectors after 10 minutes. The trend in the final contact angle was showing the lowest angle for Ti followed by Cu, Ni, Al and SS. Thus, it supports our performance and qualitative characterizations. Moreover, we also performed dynamic contact angle analysis. Here, we put 1 drop of 50 μL of the electrolyte on the current collector. We measure its initial contact angle and then the contact angle after 10 minutes. We observe no discrepancy in change of contact angle after 10 min, following the same trends observed previously, with $\Delta\theta_{Ti} > \Delta\theta_{Cu} > \Delta\theta_{Ni} > \Delta\theta_{Al} > \Delta\theta_{ss}$ (Fig. 3(B)). All the other contact angle images for the different current collectors are shown in Fig. S3(B).† A greater change in contact angle indicates higher surface wettability,[40,41] leading to more uniform Zn deposition. This argument also aligns with the performance of the current collectors in coin cell efficiency.

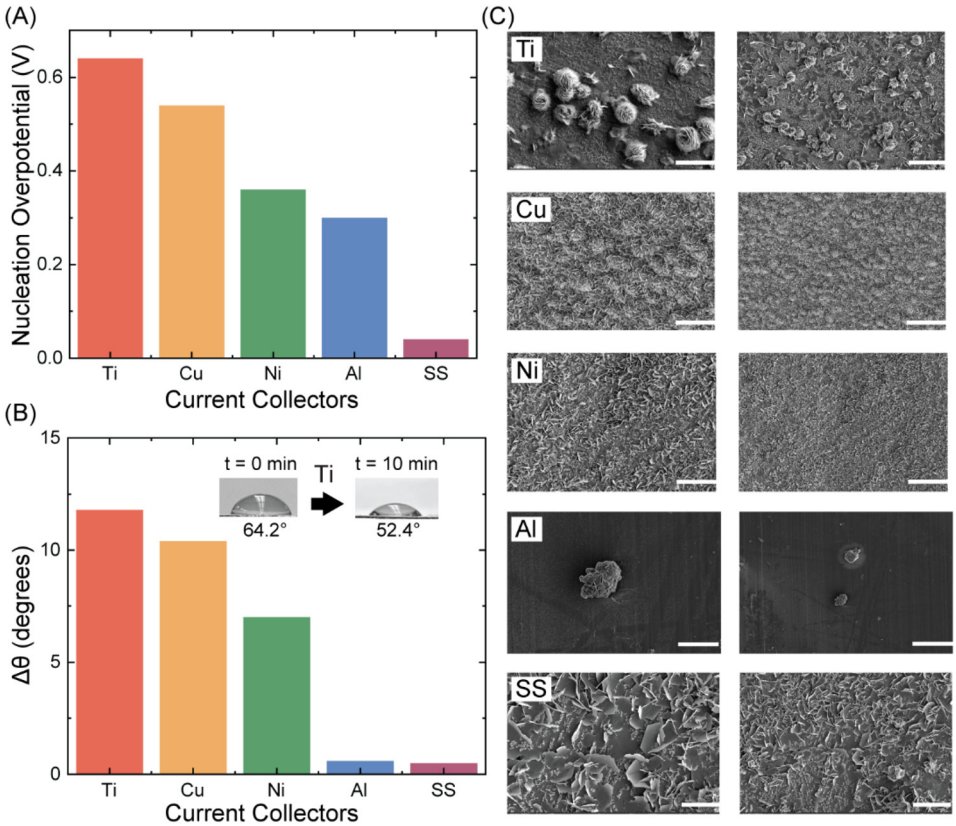

Fig. 3 (A) Nucleation overpotential for the galvanostatic plating of 0.5 mA h cm^{-2} of Zn on Cu as a function of collector materials. (B) Variation in contact angle after 10 min on the different current collectors. (C) SEM images of 0.5 mA h cm^{-2} deposited onto different current collectors. The scale bar for the panel on the left is 10 μm and for the panel on the right is 30 μm.

© 2025 The Author(s). Published by the Royal Society of Chemistry

Open Access Article. Published on 07 1446. Downloaded on 26/08/47 09:31:43 .
This article is licensed under a Creative Commons Attribution 3.0 Unported Licence.

We also evaluate the morphology of the Zn deposition using SEM. While the Zn plating on Ti exhibits a cluster-like morphology, this feature progressively diminishes when transitioning to Cu, Ni, and SS substrates, where the morphology shifts toward more flake-like structures. Flake like structures are known to be from zinc oxide or hydroxide-based side products which can hamper the performance and cyclability of the battery.[35] Ti and Cu show cluster like structures (stacking of deposited Zn orientations) which have been shown previously to be beneficial for the battery.[28,42] Thus, from this discussion of nucleation overpotential, contact angle measurements and SEM, we demonstrate how the Zn electrodeposition is more efficient for Ti and Cu compared to Ni and SS. Al shows strange morphology as we had discussed before. The next section examines side products from various side reactions and their impact on the selected current collectors.

Previously, we examined electrodeposition; here, we analyze how charge distribution to side reactions affects current collectors.[35,43] Beyond HER, corrosion and passivation also decreases the performance. Notably, Zn morphology shifts from clusters to flakes when transitioning from Ti to SS. It is also important to note here that both Zn metal and Zn side products (oxide/hydroxide) are Hexagonal Close Packed (HCP) and show hexagonal flakes. While Ti showed clusters and a lack of flaky structure, we strengthen our argument here by doing XRD of the components to detect the side products. We know from literature that high-index Zn orientations (101) and (100) correlate to deposition angles of 38–70° and 90° respectively which are known to be dendritic in nature and detrimental to the performance of the battery. And low-index Zn orientations of (002) are of deposition angles 0–37° which are known to be uniform in nature and beneficial to the performance of the battery.[34] (Deposition angles are measured relative to the substrate). Here, in Fig. 4(A) we show the XRD spectra of all our current collectors. Peaks of 002 and 100 and 101 were matched from literature values.[34,44] We compare the ratios of the different peaks observed for the current collectors to understand the Zn deposition on it. Cu(111) peak overlaps with Zn(101) peak. Therefore, along with $R_{002}/(R_{100} + R_{101} + R_{002})$ ratio we have also provided R_{002}/R_{100} ratio for all current collectors in Table S1.† We found that Ti and Cu have higher ratios than Ni and SS. This indicates that the propensity of uniform deposition is higher for Ti and Cu than Ni and SS. Ni and SS tend to show more of dendritic morphology which are more representative of the side products formed.

To analyze these side-products further, we perform Energy Dispersive X-ray (EDX) elemental mapping of Ti (best performing current collector) and SS (worst performing current collector) in Fig. 4(B). First, EDX analysis confirms the presence of sulfur-containing species on the SS electrode, likely due to interfacial reactions. In contrast, no detectable sulfur signal is observed on the Ti surface as shown in Fig. S4,† indicating a more stable interface and lower propensity for side-product accumulation which is reflected from the performance data we have discussed before. Second, it is also important to note that there are distinct blank spots (dark) seen in the EDX mapping of the substrate of Ti (rightmost), which again shows the formation of Zn clusters on Ti and flaky structures on SS. Therefore, from the XRD and SEM-EDX data of Zn on Ti is primarily from Zn metal deposition whereas Zn present on SS is

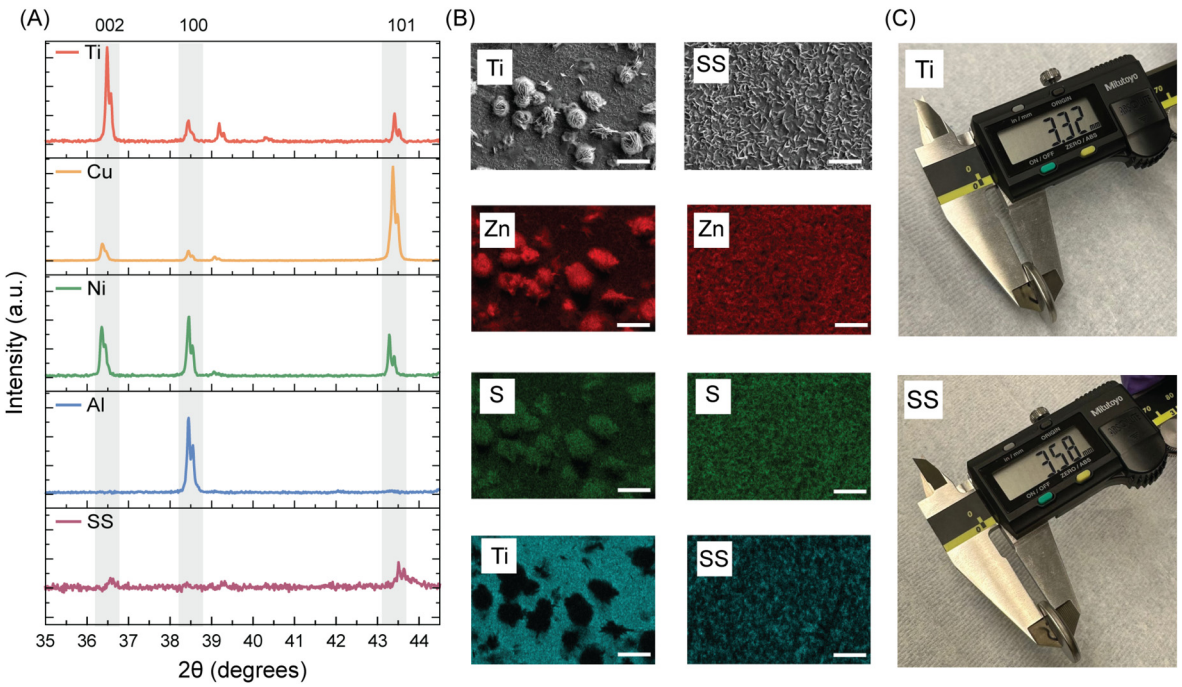

Fig. 4 (A) XRD spectra of electrodeposited Zn on different materials, at a fixed capacity of 0.5 mA h cm^{-2}. (B) SEM and EDX mapping for Ti and SS. (Scale bar: 10 μm.) (C) Thickness of Ti and SS coin cells is shown after 50 cycles.

© 2025 The Author(s). Published by the Royal Society of Chemistry

Open Access Article. Published on 07 1446. Downloaded on 26/08/47 09:31:43 .
This article is licensed under a Creative Commons Attribution 3.0 Unported Licence.

primarily from ZHS. Moreover, we observe the effect of HER in the coin cell with the different current collectors in Fig. 4(D). After 50 cycles, the thickness of the SS coin cell was appreciably higher (3.58 mm) than that of Ti (3.32 mm). This clearly depicts the heightened effect of HER for SS compared to Ti. Not only is this bad for the performance of the cell, but also the safety of using these batteries.[34] We also observe in Fig. S5† that the thickness of Zn||Cu half-cell is around 3.28 mm which is close to the thickness of Ti, signifying the higher resistance of the Zn||Cu battery to the deteriorating side reactions. This will be helpful in the upcoming discussions.

The previous sections illustrate how charge distribution between zinc electrodeposition and side reactions influences current collector performance. Titanium (Ti) and copper (Cu) promote uniform Zn deposition with lower resistance, while Ni and SS favor side reactions, causing dendritic growth, HER, corrosion, and passivation. Next, we will optimize other coin cell components, namely the spacer, spring, and case to further enhance battery performance and longevity.

Optimizing spacer, spring, and case

In addition to the current collector, other components of the coin cell such as the spacer, spring, and case also significantly influence the performance and cyclability of asymmetric aqueous zinc–metal batteries. These components are typically made of stainless steel due to its affordability. However, as demonstrated above, stainless steel is highly susceptible to side reactions during zinc electrodeposition. This raises critical concerns about the role of the spacer, spring, and case in contributing to the degradation of coin cell performance. Here, we delve deeper into this issue to understand and address these challenges.

To observe the effect of side reactions on the spacer, spring, and case, we run a Zn||Cu coin cell with 1 M $ZnSO_4$ for 50 cycles and then decrimp it. In the coin cell cases, spacer, and spring, we observe a white milky layer and a brownish stain as shown in Fig. 5(A). These are indicative of side reactions like corrosion, passivation and hydrogen evolution which are all responsible for destabilizing the cell.[29] We also performed XRD as shown in Fig. 5(B) on the spacer and got two distinct peaks (around 17 and 27 degrees) within the region of 10–30 degrees which have been known previously for the existence of ZHS side products, representing the flaky structure observed as shown in the inset (observed in SEM).[29,45,46] To get a deeper view of the side products formed, we did SEM imaging of the case, spacer and spring as shown in Fig. 5(C). We observe the formation of flakes and dendritic structures on each of the materials. Previous reports have shown how flakes are indicative of side products formed during Zn deposition and dendritic structures are responsible for shorting the cell.[35] Fresh samples of case, spring and spacer are reported in Fig. S6† for appropriate comparison. These results clearly indicate the deteriorating effect of what side products caused in the presence of stainless-steel coin cell components. In the next section, we will see how we are mitigating these effects by using a simple and cost-effective option.

In this work, to mitigate the effect of side reactions on the stainless-steel coin cell components, we add a Cu foil between Zn foil and the spacer as shown in Fig. 6(A). We observe two things from the previous current collector section: 1. Cu

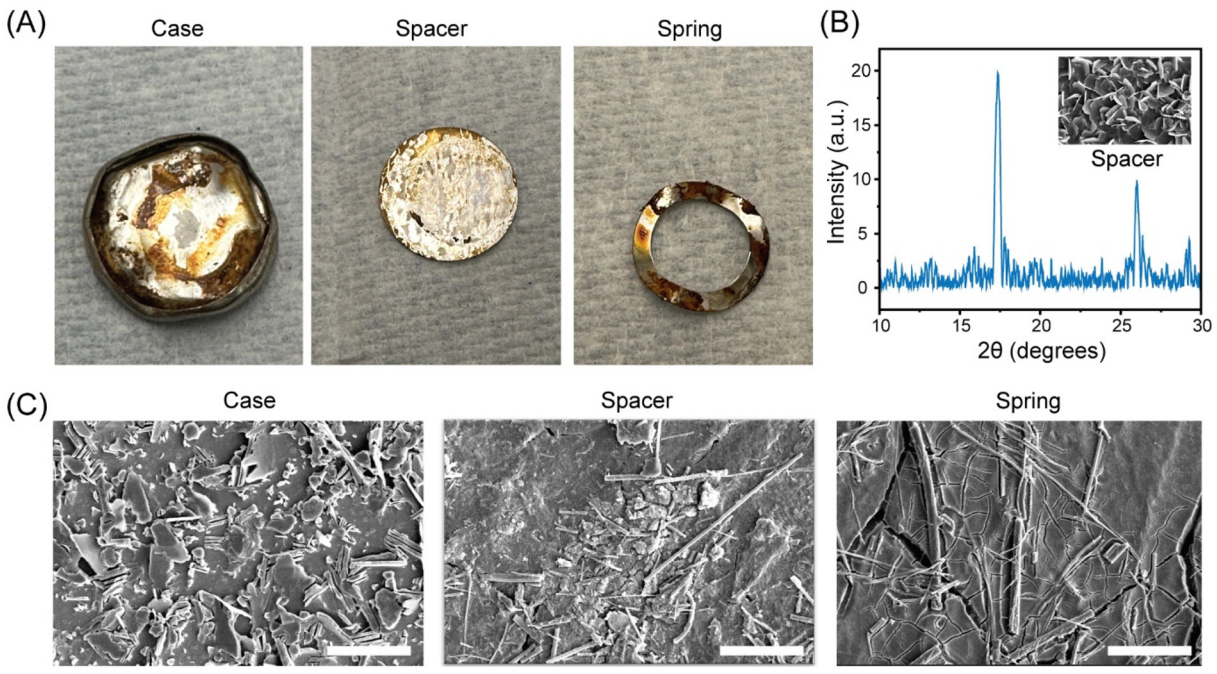

Fig. 5 (A) Case, spacer, and spring after 50 cycles of Zn||Cu coin cell. (B) XRD spectrum of the spacer (at low angles), inset shows observation in SEM of Zn deposition on SS. (C) SEM images of case, spacer, and spring after 50 cycles of Zn||Cu coin cell. (Scale bar is 10 μm.)

© 2025 The Author(s). Published by the Royal Society of Chemistry

Open Access Article. Published on 07 1446. Downloaded on 26/08/47 09:31:43 .
This article is licensed under a Creative Commons Attribution 3.0 Unported Licence.

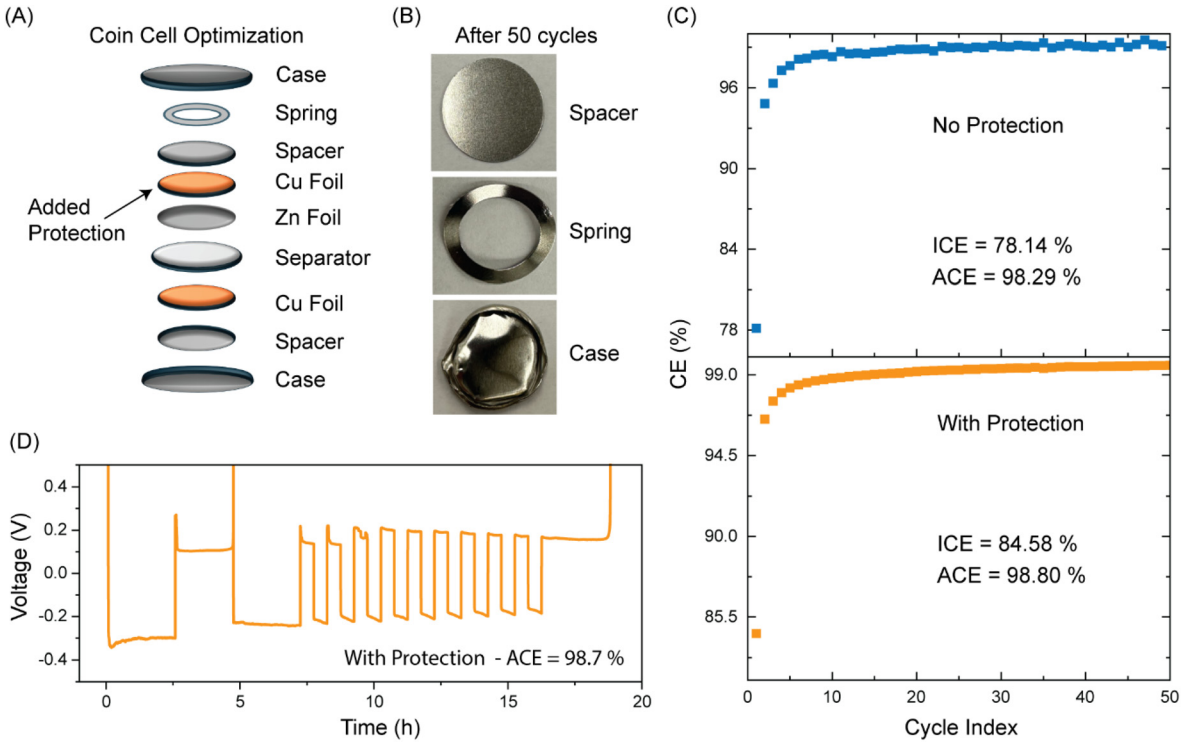

Fig. 6 (A) Schematic of the coin cell configuration with a layer of protection added. (B) Images of spacer, spring, and case after 50 cycles in a coin cell containing a protective Cu foil between Zn and the spacer. (C) The performances of Zn||Cu coin cell with (bottom) and without (top) protection are depicted. (D) Coulombic efficiency evaluation using Aurbach protocol for coin cell with protection.

attains better performance than SS and 2. Cu and Ti give similar performance, shown in our coin cell data as well as the characterizations done *via* SEM, EDX and XRD as shown in Fig. 2–4. Thus, we used Cu as a cost-effective protective foil to minimize the effect of HER, passivation and corrosion on the spacer, spring, and the case to improve the coin cell performance.

Now, with the protective Cu foil inside our coin cell, we examine its performance. Fig. 6(B) shows the images of spacer, spring, and case after 50 cycles of cycling. The coin cell was decrimped for imaging. Unlike in Fig. 5(A), there was little sign of corrosion or passivation resultant of side reactions or HER, which are known to degrade the coin cell. We show that with a protection layer, the coin cell runs much longer than without a protection layer. Without the protection layer (control), we reported around 80 cycles. But with the protection layer, it outperforms the control as shown in Fig. S7 and S9.† In terms of battery performance as well as shown in Fig. 6 (C), without the protection we observed an ICE of 78.14% and Average Coulombic Efficiency (ACE) of 98.29%, whereas with a protection layer, an ICE of 84.58% and ACE of 98.80% are achieved. We also evaluated the performance *via* Aurbach measurements as shown in Fig. 6(D) and Fig. S8.† We observed the same trend with the coin cell containing the protection giving a better performance. This argument aligns with our previous data. We know that SS gives flaky and dendritic structures as it is more prone to side reactions indicating the presence of ZHS which was depicted using SEM and XRD. On the other hand, Cu gives more uniform and homogenous deposition, which results in its better performance than SS as shown in Fig. 1. Therefore, by using a Cu protective layer above the SS spacer, the efficiency of the battery is improved through mitigating corrosion, passivation and HER on the spacer, spring, and case. The cyclability of coin cells with the protective layer and without the protection are reported in Fig. S9† confirms this observation. The coin cell with the protective layer lasts much longer than the one without the protection. This approach provides a cost-effective and efficient solution for enhancing zinc battery systems in laboratory settings. In the next section, we explored another simple yet impactful technique to further improve battery performance.

Here, we investigated the impact of varying electrolyte volumes in the coin cell. Conventionally, 150–200 μL of electrolyte is used in coin cell studies.[29] However, we questioned whether this excess electrolyte truly enhances performance, or if it may contribute to the deterioration of the cell. We tested two different volumes of 1 M $ZnSO_4$ electrolyte: 40 μL and 150 μL. We illustrated in Fig. 7(A) that the performance of the coin cell containing 40 μL of the volume performed better than the one with 150 μL. We also conducted Aurbach studies, which showed the same trend as depicted in Fig. 7(B) and (C), and Fig. S10.† The coin cell with 40 μL of electrolyte outperformed that with 150 μL. We employed a standard Zn||Cu asymmetric cell for this study. The reason for this trend can be

© 2025 The Author(s). Published by the Royal Society of Chemistry

Open Access Article. Published on 07 1446. Downloaded on 26/08/47 09:31:43 .
This article is licensed under a Creative Commons Attribution 3.0 Unported Licence.

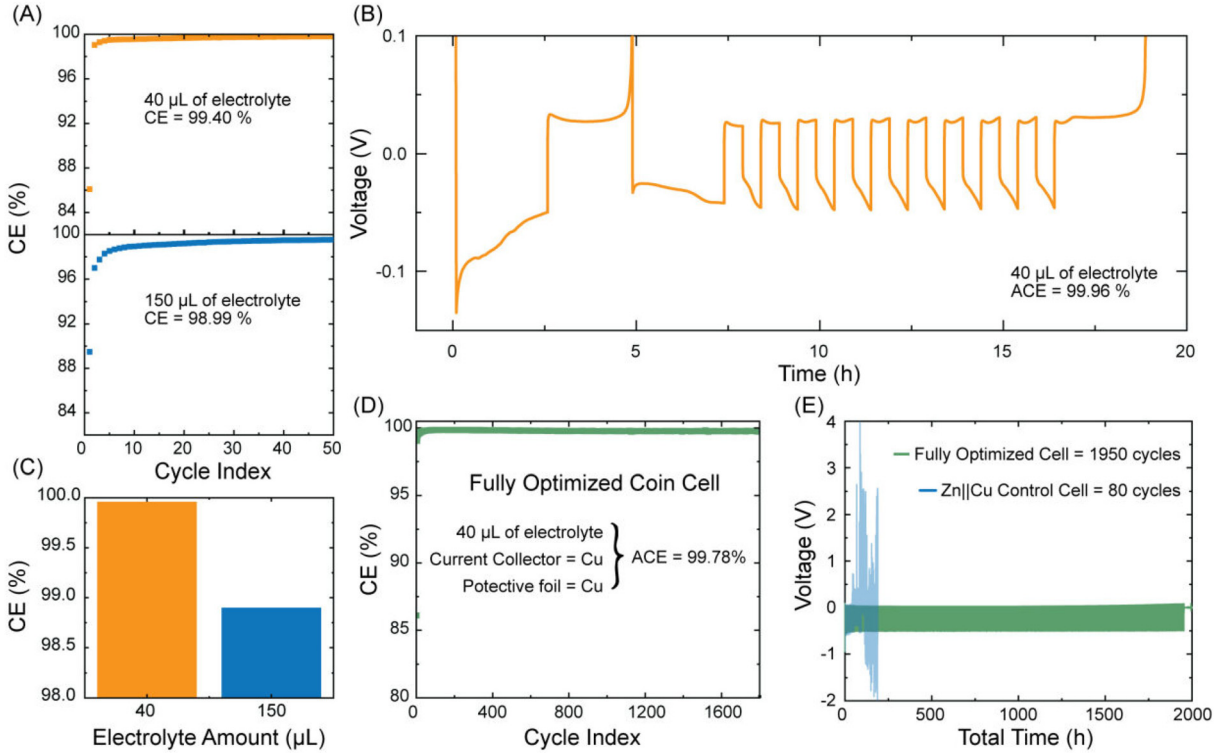

Fig. 7 (A) Coulombic efficiencies of coin cells using 40 μL and 150 μL of electrolyte in the coin cell. (B) Coulombic efficiency using Aurbach protocol for a coin cell containing 40 μL of electrolyte (C) coulombic efficiencies achieved using Aurbach protocol for 40 μL and 150 μL of electrolyte volume are shown. (D) The performance (coulombic efficiency) of a fully optimized coin cell (E) cyclability of a fully optimized coin cell (green) and a Zn||Cu (blue) cell serving as a control.

traced back in our previous discussion about side reactions and side products which is explained in our schematic as to how during the plating cycle of Zn, along with electrodeposition of Zn there are consequent side reactions that may occur. These side reactions negatively impact coin cell performance and longevity. Our data suggests that higher electrolyte volumes exacerbate these reactions, leading to greater degradation. As seen in Fig. S11,† coin cells with lower electrolyte volumes sustained a higher CE than those with higher amounts. Thus, reducing electrolyte volume offers a simple, cost-effective approach to mitigate side reactions, enhancing both performance and lifespan.

Conjointly, we made the most optimized coin cell as shown in Fig. 7(D) to explore its performance and compare it with traditional techniques. We use Cu as a current collector, insertion of Cu foil as a protective layer and using 40 μL of electrolyte to prevent degradation of the coin cell components *via* corrosion, passivation, or HER. Not only does our coin cell run at least 20 times more than our control of a standard asymmetric Zn||Cu coin cells (80 cycles *vs.* 1950 cycles), but it also shows better performance (shown in Fig. 7(E)) than standard Zn||Cu coin cells (CE of 99.3%). With all the optimizations shown in this paper, we acquired a commendable CE of 99.78%; therefore, showing the power of these simple optimization techniques. Different electrolytes like 1 M $ZnCl_2$ show similar trends with electrolyte volume, lower performance with 150 μL compared to 40 μL as shown in Fig. S12.† We have also observed that for 80 μL of $ZnSO_4$, the performance is in between that of 40 μL and 150 μL as seen in Fig. S11† going together with our previously observed trend.

This exhibits the potential of non-electrode components in the performance and cyclability of the coin cell. The coin cell components containing spacer, spring and case of the most optimized cell given in Fig. S13† look very clean and devoid of side products, like Fig. 6(B). In comparison, the coin cell components while using 150 μL seen in Fig. S13† have white patches similar to the side products seen in Fig. 5(A). Thus, the impact of simple modifications on these non-electrode components cannot be disregarded, calling for standardization of coin cell assemblies for consistency and reliability of data across different AZMB studies.

Conclusion

In this study, we highlighted the critical yet overlooked role played by non-electrode components in AZMB coin cells performances. To that effect, we demonstrated that simple and cost-effective modifications strategies significantly enhance AZMBs performance. Through systematic material screening and optimization, we identified Ti and Cu as ideal current collectors capable of considerably elongating the lifetime of the

© 2025 The Author(s). Published by the Royal Society of Chemistry

Open Access Article. Published on 07 1446. Downloaded on 26/08/47 09:31:43 .
This article is licensed under a Creative Commons Attribution 3.0 Unported Licence.

coin cells (cyclability) and coulombic efficiency. Our experiments also showed that inserting a simple protective Cu foil over stainless steel components suffices to mitigate corrosion, hydrogen evolution reaction (HER) and passivation, which are factors of hindrance towards high performance in AZMBs. In addition to the previous modifications, reducing electrolyte volume further to 40 μL leads to total improvement of 99.78% for coulombic efficiency and up to 1950 cycles life over the 99.3% and 80 cycles observed for the Zn‖Cu control. These findings demonstrate the impact of non-electrode components emphasizing the urgent need for reporting and standardization in AZMB coin cell assembly, ensuring reproducibility and meaningful performance comparisons across studies.

Author contributions

S. P. and J. H. N. contributed equally to this work. M. L. H., A. R., and A. B. helped with the experiments. J. E. D. supervised the project. All authors have agreed to the final version of the manuscript.

Data availability

The data that supports the findings of this study are available from the authors on request.

Conflicts of interest

The authors declare no competing interests.

Acknowledgements

The research was sponsored by the Army Research Office and was accomplished under grant number (W911NF-24-1-0199). The views and conclusions contained in this document are those of the authors and should not be interpreted as representing the official policies, either expressed or implied, of the Army Research Office or the U.S. Government. The U.S. Government is authorized to reproduce and distribute reprints for Government purposes notwithstanding any copyright notation herein. The authors acknowledge the use of Chat-GPT 3.5 for language refinement. The authors would also like to acknowledge the use of facilities within the Purdue Electron Microscopy Center Facility RRID SCR_022687.

References

1 B. Tang, L. Shan, S. Liang and J. Zhou, Issues and opportunities facing aqueous zinc-ion batteries, *Energy Environ. Sci.*, 2019, **12**(11), 3288–3304.
2 H. Tian, Z. Li, G. Feng, Z. Yang, D. Fox, M. Wang, H. Zhou, L. Zhai, A. Kushima and Y. Du, Stable, high-performance, dendrite-free, seawater-based aqueous batteries, *Nat. Commun.*, 2021, **12**(1), 237.
3 H. Pan, Y. Shao, P. Yan, Y. Cheng, K. S. Han, Z. Nie, C. Wang, J. Yang, X. Li and P. Bhattacharya, Reversible aqueous zinc/manganese oxide energy storage from conversion reactions, *Nat. Energy*, 2016, **1**(5), 1–7.
4 S. Higashi, S. W. Lee, J. S. Lee, K. Takechi and Y. Cui, Avoiding short circuits from zinc metal dendrites in anode by backside-plating configuration, *Nat. Commun.*, 2016, **7**(1), 11801.
5 Y. Li and J. Lu, Metal–air batteries: will they be the future electrochemical energy storage device of choice?, *ACS Energy Lett.*, 2017, **2**(6), 1370–1377.
6 D. Kundu, B. D. Adams, V. Duffort, S. H. Vajargah and L. F. Nazar, A high-capacity and long-life aqueous rechargeable zinc battery using a metal oxide intercalation cathode, *Nat. Energy*, 2016, **1**(10), 1–8.
7 O. Schmidt, A. Hawkes, A. Gambhir and I. Staffell, The future cost of electrical energy storage based on experience rates, *Nat. Energy*, 2017, **2**(8), 1–8.
8 F. Wan, X. Zhou, Y. Lu, Z. Niu and J. Chen, Energy storage chemistry in aqueous zinc metal batteries, *ACS Energy Lett.*, 2020, **5**(11), 3569–3590.
9 L. Cao, D. Li, T. Pollard, T. Deng, B. Zhang, C. Yang, L. Chen, J. Vatamanu, E. Hu and M. J. Hourwitz, Fluorinated interphase enables reversible aqueous zinc battery chemistries, *Nat. Nanotechnol.*, 2021, **16**(8), 902–910.
10 D. Han, C. Cui, K. Zhang, Z. Wang, J. Gao, Y. Guo, Z. Zhang, S. Wu, L. Yin and Z. Weng, A non-flammable hydrous organic electrolyte for sustainable zinc batteries, *Nat. Sustainability*, 2022, **5**(3), 205–213.
11 G. Feng, J. Guo, H. Tian, Z. Li, Y. Shi, X. Li, X. Yang, D. Mayerich, Y. Yang and X. Shan, Probe the localized electrochemical environment effects and electrode reaction dynamics for metal batteries using in situ 3D microscopy, *Adv. Energy Mater.*, 2022, **12**(3), 2103484.
12 H. Glatz, E. Tervoort and D. Kundu, Unveiling critical insight into the Zn metal anode cyclability in mildly acidic aqueous electrolytes: implications for aqueous zinc batteries, *ACS Appl. Mater. Interfaces*, 2019, **12**(3), 3522–3530.
13 N. Dong, F. Zhang and H. Pan, Towards the practical application of Zn metal anodes for mild aqueous rechargeable Zn batteries, *Chem. Sci.*, 2022, **13**(28), 8243–8252.
14 V. P. Hoang Huy, L. T. Hieu and J. Hur, Zn metal anodes for Zn-ion batteries in mild aqueous electrolytes: Challenges and strategies, *Nanomaterials*, 2021, **11**(10), 2746.
15 J. Huang, Z. Guo, Y. Ma, D. Bin, Y. Wang and Y. Xia, Recent progress of rechargeable batteries using mild aqueous electrolytes, *Small Methods*, 2019, **3**(1), 1800272.
16 W. Du, E. H. Ang, Y. Yang, Y. Zhang, M. Ye and C. C. Li, Challenges in the material and structural design of zinc anode towards high-performance aqueous zinc-ion batteries, *Energy Environ. Sci.*, 2020, **13**(10), 3330–3360.

© 2025 The Author(s). Published by the Royal Society of Chemistry

Open Access Article. Published on 07 1446. Downloaded on 26/08/47 09:31:43 .
This article is licensed under a Creative Commons Attribution 3.0 Unported Licence.

17 J. Yang, B. Yin, Y. Sun, H. Pan, W. Sun, B. Jia, S. Zhang and T. Ma, Zinc anode for mild aqueous zinc-ion batteries: challenges, strategies, and perspectives, *Nano-Micro Lett.*, 2022, **14**, 1–47.
18 X. Yu, Z. Li, X. Wu, H. Zhang, Q. Zhao, H. Liang, H. Wang, D. Chao, F. Wang and Y. Qiao, Ten concerns of Zn metal anode for rechargeable aqueous zinc batteries, *Joule*, 2023, **7**(6), 1145–1175.
19 L. Kang, M. Cui, F. Jiang, Y. Gao, H. Luo, J. Liu, W. Liang and C. Zhi, Nanoporous $CaCO_3$ coatings enabled uniform Zn stripping/plating for long–life zinc rechargeable aqueous batteries, *Adv. Energy Mater.*, 2018, **8**(25), 1801090.
20 X. Zeng, J. Hao, Z. Wang, J. Mao and Z. Guo, Recent progress and perspectives on aqueous Zn-based rechargeable batteries with mild aqueous electrolytes, *Energy Storage Mater.*, 2019, **20**, 410–437.
21 P. Zou, R. Zhang, L. Yao, J. Qin, K. Kisslinger, H. Zhuang and H. L. Xin, Ultrahigh–rate and long–life zinc–metal anodes enabled by self–accelerated cation migration, *Adv. Energy Mater.*, 2021, **11**(31), 2100982.
22 B. K. Thomas and D. J. Fray, The effect of additives on the morphology of zinc electrodeposited from a zinc chloride electrolyte at high current densities, *J. Appl. Electrochem.*, 1981, **11**(6), 677–683.
23 J. Cui, Z. Li, A. Xu, J. Li and M. Shao, Confinement of zinc salt in ultrathin heterogeneous film to stabilize zinc metal anode, *Small*, 2021, **17**(28), 2100722.
24 Y. Dou, Y. Wang, D. Tian, J. Xu, Z. Zhang, Q. Liu, B. Ruan, J. Ma, Z. Sun and S. X. Dou, Atomically thin Co3O4 nanosheet-coated stainless steel mesh with enhanced capacitive Na+ storage for high-performance sodium-ion batteries, *2D Mater.*, 2016, **4**(1), 015022.
25 A. Kayyar, J. Huang, M. Samiee and J. Luo, Construction and testing of coin cells of lithium ion batteries, *J. Visualized Exp.*, 2012, (66), 4104.
26 N. N. Sinha, J. C. Burns, R. J. Sanderson and J. Dahn, Comparative studies of hardware corrosion at high potentials in coin-type cells with non aqueous electrolytes, *J. Electrochem. Soc.*, 2011, **158**(12), A1400.
27 N. Harpak, G. Davidi and F. Patolsky, Self-transforming stainless-steel into the next generation anode material for lithium ion batteries, *J. Energy Chem.*, 2022, **64**, 432–441.
28 U. Mittal and D. Kundu, Electrochemical stability of prospective current collectors in the sulfate electrolyte for aqueous Zn-ion battery application, *J. Electrochem. Soc.*, 2021, **168**(9), 090560.
29 G. Wu, Y. Yang, R. Zhu, W. Yang, H. Yang and H. Zhou, The pitfalls of using stainless steel (SS) coin cells in aqueous zinc battery research, *Energy Environ. Sci.*, 2023, **16**(10), 4320–4325.
30 H. Li, W. Jia, P. Chen, L. Wang, X. Yan and Y.-Y. Yang, Zinc deposition characteristics on different substrates for aqueous zinc ion battery, *Appl. Surf. Sci.*, 2023, **607**, 155111.
31 L. Ma, M. A. Schroeder, O. Borodin, T. P. Pollard, M. S. Ding, C. Wang and K. Xu, Realizing high zinc reversibility in rechargeable batteries, *Nat. Energy*, 2020, **5**(10), 743–749.
32 B. D. Adams, J. Zheng, X. Ren, W. Xu and J. G. Zhang, Accurate determination of coulombic efficiency for lithium metal anodes and lithium metal batteries, *Adv. Energy Mater.*, 2018, **8**(7), 1702097.
33 K. Roy, A. Rana, J. N. Heil, B. M. Tackett and J. E. Dick, For Zinc Metal Batteries, How Many Electrons go to Hydrogen Evolution? An Electrochemical Mass Spectrometry Study, *Angew. Chem.*, 2024, **136**(11), e202319010.
34 K. Roy, A. Rana, T. K. Ghosh, J. N. Heil, S. Roy, K. J. Vannoy, B. M. Tackett, M. Chen and J. E. Dick, How Solvation Energetics Dampen the Hydrogen Evolution Reaction to Maximize Zinc Anode Stability, *Adv. Energy Mater.*, 2024, **14**(15), 2303998.
35 A. Rana, K. Roy, J. N. Heil, J. H. Nguyen, C. Renault, B. M. Tackett and J. E. Dick, Realizing the Kinetic Origin of Hydrogen Evolution for Aqueous Zinc Metal Batteries, *Adv. Energy Mater.*, 2024, **14**(43), 2402521.
36 X. Jia, C. Liu, Z. G. Neale, J. Yang and G. Cao, Active materials for aqueous zinc ion batteries: synthesis, crystal structure, morphology, and electrochemistry, *Chem. Rev.*, 2020, **120**(15), 7795–7866.
37 Q. Li, A. Chen, D. Wang, Y. Zhao, X. Wang, X. Jin, B. Xiong and C. Zhi, Tailoring the metal electrode morphology via electrochemical protocol optimization for long-lasting aqueous zinc batteries, *Nat. Commun.*, 2022, **13**(1), 3699.
38 W. Nie, H. Cheng, Q. Sun, S. Liang, X. Lu, B. Lu and J. Zhou, Design strategies toward high–performance Zn metal anode, *Small Methods*, 2024, **8**(6), 2201572.
39 A. J. Bard, L. R. Faulkner and H. S. White, *Electrochemical methods: fundamentals and applications*, John Wiley & Sons, 2022.
40 S. Paul, J. Reyes-Morales, K. Roy and J. E. Dick, Anodic Electrodeposition of IrO x Nanoparticles from Aqueous Nanodroplets, *ACS Nanosci. Au*, 2024, **4**(3), 216–222.
41 J. Reyes-Morales, S. Paul, M. Vullo, M. Q. Edwards and J. E. Dick, Room Temperature Electrochemical-Shock Synthesis of Solid-Solution Medium-Entropy Alloy Nanoparticles for Hydrogen Evolution, *Langmuir*, 2024, **40**(46), 24272–24280.
42 Z. Wang, J. Wang, K. Kawashima, Z. Liu, G. Henkelman and C. B. Mullins, Mass Transfer Limitation within Molecular Crowding Electrolyte Reorienting (100) and (101) Texture for Dendrite-Free Zinc Metal Batteries, *Angew. Chem., Int. Ed.*, 2024, **63**(34), e202407881.
43 A. Rana, M. A. Faisal, K. Roy, J. H. Nguyen, S. Paul and J. E. Dick, How the Kinetic Balance Between Charge–Transfer and Mass–Transfer Influences Zinc Anode Stability: An Ultramicroelectrode Study, *Small Methods*, 2024, 2401021.
44 K. Zhao, C. Wang, Y. Yu, M. Yan, Q. Wei, P. He, Y. Dong, Z. Zhang, X. Wang and L. Mai, Ultrathin surface coating enables stabilized zinc metal anode, *Adv. Mater. Interfaces*, 2018, **5**(16), 1800848.

© 2025 The Author(s). Published by the Royal Society of Chemistry

45 K. Huang, X. Zeng, D. Zhang, Y. Wang, M. Lan, C. Wen and Y. Guo, Tailoring crystallization zinc hydroxide sulfates growth towards stable zinc deposition chemistry, *Nano Res.*, 2024, **17**(6), 5243–5250.

46 Z. Xiang, Y. Qiu, X. Guo, K. Qi, Z.-L. Xu and B. Y. Xia, Inherited construction of porous zinc hydroxide sulfate layer for stable dendrite-free Zn anode, *Energy Environ. Sci.*, 2024, **17**(10), 3409–3418.

Open Access Article. Published on 07 1446. Downloaded on 26/08/47 09:31:43 .
This article is licensed under a Creative Commons Attribution 3.0 Unported Licence.